

Universal Statistics of Branched Flows

Jakob J. Metzger,^{1,2} Ragnar Fleischmann,¹ and Theo Geisel^{1,2}

¹Max-Planck-Institute for Dynamics and Self-Organization, Bunsenstr a e 10, 37073 G ottingen, Germany

²Institute for Nonlinear Dynamics, Department of Physics, University of G ottingen, 37077 G ottingen, Germany

(Received 19 December 2009; published 7 July 2010)

Even very weak correlated disorder potentials can cause extreme fluctuations in Hamiltonian flows. In two dimensions this leads to a pronounced branching of the flow. Although present in a great variety of physical systems, a quantitative theory of the branching statistics is lacking. Here, we derive an analytical expression for the number of branches valid for all distances from a source. We also derive the scaling relations that make this expression universal for a wide range of random potentials. Our theory has possible applications in many fields ranging from semiconductor to geophysics.

DOI: 10.1103/PhysRevLett.105.020601

PACS numbers: 05.40.-a, 42.25.Dd, 73.23.-b

Conservative particle or wave flows can be strongly influenced by very weak, smooth disorder potentials. A prominent example is the electron flow in the two-dimensional electron gas of high mobility semiconductor heterostructures at low temperatures. Even though impurity scattering in these systems only leads to small-angle deflections in the individual electron paths, the electron flow can become strongly branched on length scales much shorter than the mean free path [1]. This branching is caused by the formation of random caustics in an initially homogeneous flow [2]. In two dimensions, caustics usually come in pairs, which constitute two focal lines emerging from a cusp point, forming a branch (cf. Fig. 1). Any flow that can be approximated by Hamiltonian dynamics and that is subject to the forces of a correlated weak random potential will exhibit the formation of random caustics. Thus branching is a wide spread effect which dominates in the spatial regime between ballistic and diffusive motion. Branched flow has been observed on length scales ranging from a few micrometers, affecting the transport properties of semiconductor and microwave devices [1,3–5], up to several thousand kilometers, influencing the sound propagation in the oceans [6]. Branching and random caustics have also been used to explain the appearance of freak ocean waves [7–9] and the activation of rain showers in turbulent clouds [10].

In this Letter, we study the statistics of branches in two-dimensional Hamiltonian systems with smooth correlated disorder. We answer the fundamental question of how many random caustics exist on average per unit length at a certain distance away from the source [cf. Fig. 1(a)]. This question was first asked and answered for the much simpler system of the free ray dynamics of an initially distorted optical wave front by Berry and Upstill [11]. For the dynamics in a continuous random potential it has only been addressed for distances far away from the source [2], where the number of caustics grows exponentially and individual branches become less visible. Here, we present an explicit analytical expression which is valid for all distances from the source. Furthermore, we show

that by a nontrivial scaling relation the branch count function can be described by a single universal curve. This curve is valid for a very wide range of random potentials, which not only differ in strength and spatial scale, but also in their type of correlations. We verify our theory by extensive numerical simulations.

Figure 1 illustrates a typical Hamiltonian flow in a correlated disorder potential. These systems are generi-

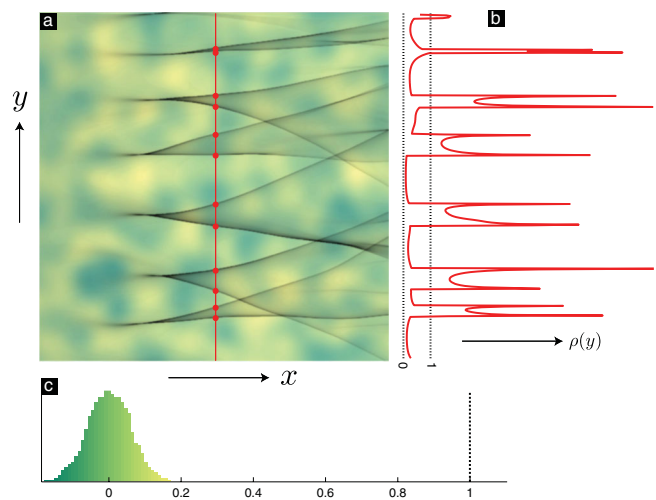


FIG. 1 (color). (a) Branched flow (dark gray is high intensity) from a plane source, caused by a weak disorder potential (low potential in green, high potential in yellow, with standard deviation $\epsilon = 6\%$ of the kinetic energy of the particles). We want to count the number of branches per unit length (along the red line) at some distance away from the source. The number of branches is (to a very good approximation) equal to half the number of caustics (red dots). (b) Intensity profile $\rho(y)$ along the red line. Branches, bounded by two caustics and with an increased density in the region between them, show up clearly. The initial density is normalized to one, which is drawn as a dashed black line, together with a line for zero density. (c) Histogram of the values of the random potential used in (a) with the same color code. The potential is clearly very weak compared to the energy of the flow, which is here normalized to one (indicated by the dashed vertical line).

cally modeled by a Hamiltonian $H = \mathbf{p}^2/2 + V(x, y)$, where \mathbf{p} is the momentum and where the potential is a Gaussian random field with zero mean $\langle V(\mathbf{r}) \rangle = 0$ with $\mathbf{r} = (x, y)$ and a two-parameter correlation function of the form $c(\mathbf{r}) = \langle V(\mathbf{r}')V(\mathbf{r}' + \mathbf{r}) \rangle = \epsilon^2 g(|\mathbf{r}|/\ell_c)$. The angular brackets denote an ensemble average over disorder realizations. Here, ℓ_c describes the correlation length and ϵ the strength of the random potential V . We note that, since ℓ_c is the only length scale in the Hamiltonian, our results are independent of a rescaling of ℓ_c . We choose to retain ℓ_c in all expressions for clarity and in order to allow for easier application of our results. The form g of the correlation is arbitrary except for smoothness and integrability conditions which are discussed later. We use the classical analog of a plane wave initial condition, i.e., particles moving initially with equal velocity in the x direction and zero velocity in the transverse y direction. The total energy of the particles is $E_0 = 1/2$, which corresponds to a mean velocity of $v_0 = 1$. Since we assume that the potential is weak (up to approximately $\epsilon \approx 10\%$ of E_0) the particles can be assumed to move fast in the x direction. This corresponds to small-angle scattering of the flow particles and allows an approximate quasi-2D treatment in which x is identified with t . The validity of this approximation is confirmed by numerical simulations.

After traversing a distance of several correlation lengths of the disorder, the cumulative deflection by the random potential has the effect of generating caustics, i.e., regions of very high intensity in the flow, which appear as branches. Since a branch is always bounded by two caustics, we proceed by giving the number of branches per unit length $N_b(t)$ as half the number of caustics. It is given by

$$N_b(t) = \frac{1}{2} \lim_{L \rightarrow \infty} \frac{1}{L} \left\langle \int_0^L dy_0 \delta(m(t)) |\partial_{y_0} m(t)| \right\rangle, \quad (1)$$

where $m(t)$ is a function (specified below) which is zero when a caustic is encountered. Equation (1) is equivalent to the expression used in [11] to calculate the number of caustics for a corrugated optical wave front which propagates through free space. In our case, we need to introduce several approximations in order to treat this expression analytically. First, we introduce the time it takes to travel along a trajectory to reach a caustic t_c and change the expression to

$$N_b(t) = \frac{1}{2} \lim_{L \rightarrow \infty} \frac{1}{L} \left\langle \int_0^L dy_0 \frac{\delta(t - t_c)}{|m(t)|} |\partial_{y_0} m(t)| \right\rangle, \quad (2)$$

which will later allow us to use the probability to reach a caustic along a trajectory, $P_c(t) = \langle \delta(t - t_c) \rangle$, which is known from the literature. We proceed by analyzing the statistical properties of $m(t)$ and $n(t) \equiv \partial_{y_0} m(t)$. The function $m(t)$ is the matrix element $i = j = 1$ of the stability matrix $\partial \gamma_i(t)/\partial \gamma_j(0)$, where γ_i is a phase space variable and γ_1 is the first spatial coordinate [12]. In the quasi-2D approach, there is only one spatial coordinate, denoted by y . The function $m(t) = \partial y(t)/\partial y(0)$ vanishes when a caus-

tic is encountered, just as we require. Similarly, $n(t)$ is defined as the first component ($i = j = k = 1$) of the extended stability tensor $\partial^2 \gamma_i(t)/(\partial \gamma_j(0) \partial \gamma_k(0))$. With $\mathbf{a} = (m, \dot{m}, n, \dot{n})$ we can calculate the equations of motion for \mathbf{a} using the Hamiltonian given above as

$$\begin{aligned} \dot{a}_1(t) &= a_2(t), & a_1(0) &= 1, \\ \dot{a}_2(t) &= -\partial_{yy} V(t, y) a_1(t), & a_2(0) &= 0, \\ \dot{a}_3(t) &= a_4(t), & a_3(0) &= 0, \\ \dot{a}_4(t) &= -\partial_{yy} V(t, y) a_3(t) - \partial_{yyy} V(t, y) a_1(t)^2, & a_4(0) &= 0. \end{aligned}$$

A Fokker-Planck equation for the probability density of \mathbf{a} can be derived in the quasi-2D approach as

$$\begin{aligned} \partial_t P(\mathbf{a}, t | \mathbf{a}', t') &= [-a_2 \partial_{a_1} - a_4 \partial_{a_3} + \sigma_1^2 a_1^2 \partial_{a_2 a_2} \\ &+ 2\sigma_1^2 a_1 a_3 \partial_{a_2 a_4} + \partial_{a_4 a_4} (\sigma_2^2 a_4^4 \\ &+ \sigma_1^2 a_3^2)] P(\mathbf{a}, t | \mathbf{a}', t'), \end{aligned} \quad (3)$$

where $\sigma_1^2 = \frac{1}{2} \int_{-\infty}^{\infty} dx \frac{\partial^4 c(x, y)}{\partial y^4} |_{y=0}$ and $\sigma_2^2 = -\frac{1}{2} \times \int_{-\infty}^{\infty} dx \frac{\partial^6 c(x, y)}{\partial y^6} |_{y=0}$ (calculated using stochastic integration methods [13]). Equation (3) cannot be solved in general. However, from this equation, we can obtain a closed set of differential equations for the moments of the components of \mathbf{a} , which are linear and can easily be solved. In this way, we obtain the second moment of $m = a_1$ as

$$\langle m^2(t) \rangle = \frac{1}{3} [e^{2\kappa t} + 2e^{-\kappa t} \cos(\sqrt{3}\kappa t)], \quad (4)$$

with $\kappa = (\sigma_1/\sqrt{2})^{2/3}$, which has been previously derived using different methods [14]. The second moment of $n = a_3$ is calculated analogously; the result is

$$\begin{aligned} \langle n^2(t) \rangle &= \frac{\sigma_2^2}{210\sigma_1^2} \{98e^{-\kappa t} \cos(\sqrt{3}\kappa t) + 49e^{2\kappa t} + e^{21^{1/3}2\kappa t} \\ &+ 2e^{-21^{1/3}\kappa t} \cos[(7 \times 3^{5/2})^{1/3} \kappa t] - 150\}. \end{aligned} \quad (5)$$

We note that the expressions for the moments are only exact in the limit $\epsilon \rightarrow 0$; however, the comparison between theory and simulations shows good agreement for the whole range of ϵ considered here. An example is shown in Fig. 2(a).

Next, we require an expression for the probability to reach a caustic along a trajectory, $P_c(t)$. We construct a compound solution from results obtained by White and co-workers [15–17] by using their approximation for small t and by using the long-time approximation of

$$P_c(t) = 1/[6.27(2\sigma_1^2)^{-1/3}] = 1/t_0, \quad (6)$$

where t_0 is the mean time (or distance) between two caustics. We will use t_0 as a time scale. Note that this differs from the time scale in the literature, $t_0 = \epsilon^{-2/3} \ell_c$ (e.g., in [2]) by a prefactor which depends on σ_1 . This allows us to treat different correlation functions. For completeness, we state the full expression for $P_c(t)$ here:

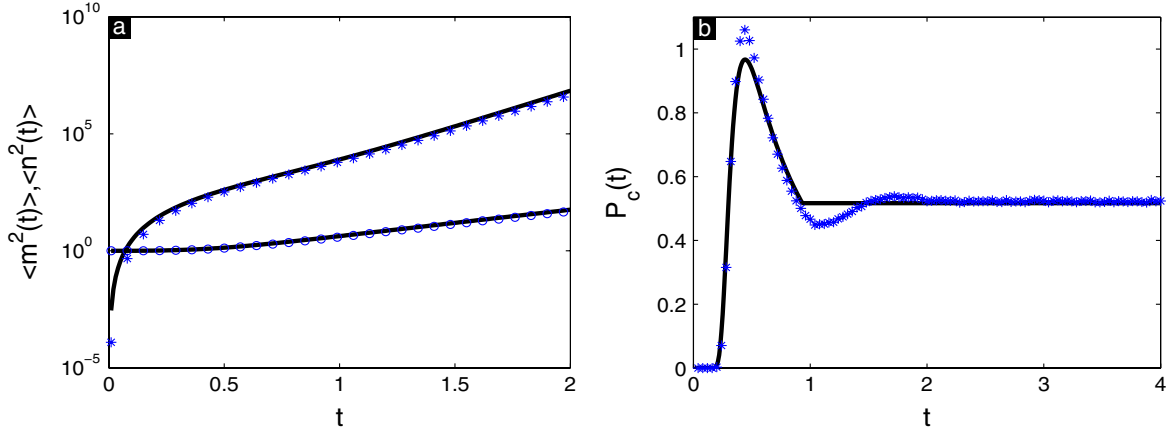


FIG. 2 (color online). (a) Second moments of $m(t)$ (circles are numerical values, solid line is the analytical prediction) and $n(t)$ (stars are numerical values, solid line is the analytical prediction). (b) Probability to reach a caustic along a trajectory $P_c(t)$, numerical calculation (stars) and composite analytical solution (solid line). All calculations in this figure are performed using an ensemble of Gaussian correlated disorder potentials with $\epsilon = 0.04E_0$ and $\ell_c = 0.1$.

$$P_c(t) = \begin{cases} [\beta^2(4\pi\sigma_1^2)^{-1/2}t^{-5/2} + C_F(2\sigma_1^2)^{1/3}]e^{-\lambda_1(2\sigma_1^2)^{1/3}t - \beta^4/(12\sigma_1^2t^3)} & \text{if } t \leq t_1 \\ 1/t_0 & \text{if } t > t_1, \end{cases} \quad (7)$$

where t_1 is the value at which the solution for small times drops below the long-term solution, $1/t_0$, and where $\beta \approx 1.854$, $\lambda_1 \approx 0.281$, $C_F \approx 0.314$. We compare the analytical solution Eq. (7) to numerical simulations in Fig. 2(b).

We now turn to evaluating Eq. (2). This will be done by construction of a short-time and a long-time approximation. For short times compared to t_0 we approximate $\langle |\dot{m}(t)| \rangle \propto 1/t_0$ at the caustics. We also assume $\langle |n(t)| \rangle$ to be statistically independent and (up to a factor) well approximated by $\sqrt{\langle n^2(t) \rangle}$. These approximations have been confirmed numerically. We can then write

$$N_b^{\text{short}}(t) \approx c_1 t_0 P_c(t) \sqrt{\langle n^2(t) \rangle}, \quad t < t_0. \quad (8)$$

Note that $n(t)$ has units of inverse length because of the prefactor σ_2/σ_1 of Eq. (5), which is proportional to $1/\ell_c$. It also encodes the dependence on different types of correlation functions, since it varies for different functional forms of the correlation function. The constant c_1 does not depend on the random potential and is determined numerically to be $c_1 \approx 0.033$.

For the long-term asymptotics, we assume \dot{m} and n to be statistically independent and the mean of their absolute value, like their even moments, to be growing exponentially. Since $P_c \approx \text{const}$ for large t , the exponent λ of $|n/\dot{m}|$ must be equal to the one obtained in [2,18,19]. The scaling with σ_2/σ_1 is the same as in the short-time solution. We therefore give the long-time asymptotics of the number of branches as

$$N_b^{\text{long}}(t) \approx c_2 (\sigma_2/\sigma_1) t_0 P_c(t) e^{\lambda(t/t_0)}, \quad t \geq t_0, \quad (9)$$

with $\lambda \approx 2.87$, which differs from the value used in [2,18,19] because of our definition of t_0 [Eq. (6)]. We numerically determine the constant $c_2 \approx 0.040$.

Since both approximations overestimate N_b in the regions where they are not applicable, we can construct a compound solution by always choosing the one that gives a lower value. The result is then given by

$$N_b(t) = \begin{cases} N_b^{\text{short}}(t) & \text{if } N_b^{\text{short}}(t) \leq N_b^{\text{long}}(t) \\ N_b^{\text{long}}(t) & \text{if } N_b^{\text{short}}(t) > N_b^{\text{long}}(t). \end{cases} \quad (10)$$

From this equation, we observe that rescaling the number of branches with σ_2/σ_1 and the time with t_0 , the resulting curve is *universal* in the sense that it is independent of the parameters of the random potential and independent of the particular functional form of the correlation function.

We have performed extensive numerical simulations to confirm our theory, using a range of values for the parameters ϵ and ℓ_c and several different correlation functions. We note that for our theory we require σ_1 and σ_2 to be finite. This implies that the correlation function has to be 6 times

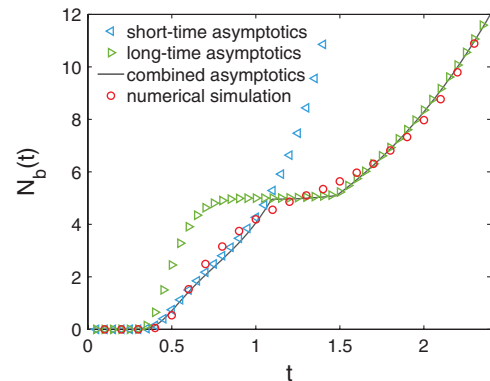


FIG. 3 (color online). Short- and long-term asymptotics as well as compound solution of $N_b(t)$, numerical data for $\epsilon = 0.04E_0$ and with $\ell_c = 0.1$.

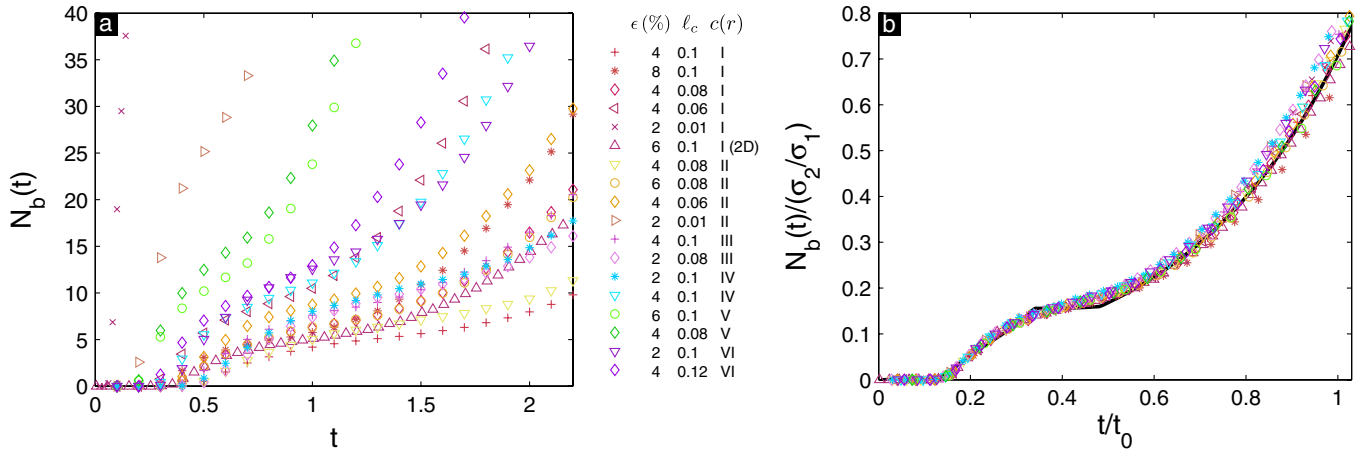


FIG. 4 (color online). (a) Number of branches $N_b(t)$ for different sets of parameters of the random potential (ϵ in percent of the total particle energy), different correlation functions, and with a fully two-dimensional simulation (2D). We note again that t corresponds to the distance away from the source. The type of correlation function is indicated by Roman numerals: Gaussian (I), exponential (II), and power law with $\alpha = 1, 2, 3, 4$ (III, IV, V, VI) (cf. text for details). (b) Same curves as in (a), but t scaled by t_0 and $N_b(t)$ by σ_2/σ_1 , together with analytical prediction (solid black line).

differentiable at the origin and that the integrals defining σ_1 and σ_2 have to be finite. These conditions are fulfilled by most standard correlation functions of smooth potentials. Here, we simulate potentials of Gaussian type [$c(\mathbf{r}) = c(r) = \epsilon^2 \exp(-r^2/\ell_c^2)$] as well as correlation functions with exponential [$c(r) = \epsilon^2 \text{sech}(r/\ell_c)$] and with power-law decays [$c(r) = \epsilon^2(1 + r^2/\ell_c^2)^{-\alpha}$ for $\alpha = 1, 2, 3, 4$]. In Fig. 3, we compare the approximations Eqs. (8) and (9), the compound solution Eq. (10), and numerical data from one set of parameters of the random potential.

Simulations for the different correlation functions and different sets of the parameters of the random potentials, ϵ and ℓ_c , are shown in Fig. 4(a). The same curves, this time scaled in both axes, are shown again in Fig. 4(b). All curves collapse onto our theoretical prediction. Also included are data from a fully two-dimensional simulation, which fit the quasi-2D simulations and the theoretical prediction equally well.

In conclusion, we have given an expression for the number of branches that a flow develops in a random potential for all distances from the source by construction and combination of two asymptotic solutions. We have shown that, by correct scaling, there is one universal curve for the number of branches. The time axis has to be scaled by t_0 , which depends on the parameters and the functional form of the correlation function. This corresponds to a typical spatial scale proportional to $\ell_c \epsilon^{-2/3}$, which is for small ϵ well separated from the scale of the mean free path, $\ell_c \epsilon^{-2}$. The scaling of $N_b(t)$ depends nontrivially on integrals of the correlation function via σ_2/σ_1 . Our results offer fundamental insights into the way different correlation functions of random potentials affect transport in weakly random media and can be applied to the great

variety of physical systems in which branched flow is observed.

This work has been supported by the DFG research group 760.

-
- [1] M. A. Topinka *et al.*, *Nature (London)* **410**, 183 (2001).
 - [2] L. Kaplan, *Phys. Rev. Lett.* **89**, 184103 (2002).
 - [3] M. P. Jura *et al.*, *Nature Phys.* **3**, 841 (2007).
 - [4] K. E. Aidala *et al.*, *Nature Phys.* **3**, 464 (2007).
 - [5] R. Höhmann *et al.*, *Phys. Rev. Lett.* **104**, 093901 (2010).
 - [6] M. Wolfson and S. Tomsovic, *J. Acoust. Soc. Am.* **109**, 2693 (2001).
 - [7] M. V. Berry, *New J. Phys.* **7**, 129 (2005).
 - [8] M. V. Berry, *Proc. R. Soc. A* **463**, 3055 (2007).
 - [9] E. J. Heller, L. Kaplan, and A. Dahlen, *J. Geophys. Res.* **113**, C09023 (2008).
 - [10] M. Wilkinson, B. Mehlig, and V. Bezuglyy, *Phys. Rev. Lett.* **97**, 048501 (2006).
 - [11] M. V. Berry and C. Upstill, *Prog. Opt.* **18**, 257 (1980).
 - [12] E. J. Heller, in *Chaos and Quantum Physics*, edited by M.-J. Giannoni, A. Voros, and J. Zinn-Justin (Elsevier Science, Amsterdam, 1991), pp. 549–663.
 - [13] G. C. Papanicolaou and W. Kohler, *Commun. Pure Appl. Math.* **27**, 641 (1974).
 - [14] M. Wolfson and F. Tappert, *J. Acoust. Soc. Am.* **107**, 154 (2000).
 - [15] V. Kulkarny and B. White, *Phys. Fluids* **25**, 1770 (1982).
 - [16] B. S. White, *SIAM J. Appl. Math.* **44**, 127 (1984).
 - [17] B. S. White and B. Fornberg, *J. Fluid Mech.* **355**, 113 (1998).
 - [18] I. L. Aleiner and A. I. Larkin, *Phys. Rev. B* **54**, 14423 (1996).
 - [19] H. Schomerus and M. Titov, *Phys. Rev. E* **66**, 066207 (2002).